Tree Physiology 21, 777–787

Leaf area distribution and radiative transfer in open-canopy forests: implications for mass and energy exchange

BEVERLY E. LAW,[1] ALESSANDRO CESCATTI[2] and DAVID D. BALDOCCHI[3]

[1] *Department of Forest Science, 328 Richardson Hall, Oregon State University, Corvallis, OR 97331, USA*

[2] *Centro di Ecologia Alpina, I-38040 Viote del Monte Bondone (TN), Italy*

[3] *Department of Environmental Science, Policy and Management, 151 Hilgard Hall, University of California, Berkeley, CA 94720, USA*

Received August 18, 2000

Summary Leaf area and its spatial distribution are key canopy parameters needed to model the radiation regime within a forest and to compute the mass and energy exchange between a forest and the atmosphere. A much larger proportion of available net radiation is received at the forest floor in open-canopy forests than in closed-canopy forests. The proportion of ecosystem water vapor exchange (λE) and sensible heat exchange from the forest floor is therefore expected to be larger in open-canopy forests than in closed-canopy forests.

We used a combination of optical and canopy geometry measurements, and robust one- and three-dimensional models to evaluate the influence of canopy architecture and radiative transfer on estimates of carbon, water and energy exchange of a ponderosa pine (*Pinus ponderosa* Dougl. *ex* Laws.) forest. Three-dimensional model simulations showed that the average probability of diffuse and direct radiation transmittance to the forest floor was greater than if a random distribution of foliage had been assumed. Direct and diffuse radiation transmittance to the forest floor was 28 and 39%, respectively, in the three-dimensional model simulations versus 23 and 31%, respectively, in the one-dimensional model simulations. The assumption of randomly distributed foliage versus inclusion of clumping factors in a one-dimensional, multi-layer biosphere-atmosphere gas exchange model (CANVEG) had the greatest effect on simulated annual net ecosystem exchange (NEE) and soil evaporation. Assuming random distribution, NEE was 41% lower, net photosynthesis 3% lower, total λE 10% lower, and soil evaporation 40% lower. The same comparisons at LAI 5 showed a similar effect on annual NEE estimates (37%) and λE (12%), but a much larger effect on net photosynthesis (20%), suggesting that, at low LAI, canopies are mostly sunlit, so that redistribution of light has little effect on net photosynthesis, whereas the effect on net photosynthesis is much greater at high LAIs.

Keywords: CANVEG, canopy architecture, carbon exchange, Pinus ponderosa, modeling.

Introduction

Leaf area and its spatial distribution play an important role in controlling energy, carbon, and water vapor exchange between forests and the atmosphere. Seasonal and diurnal changes in solar zenith angle result in different exposures of open canopies to sunlight and shadows, which in turn influences carbon uptake, transpiration, energy partitioning (Baldocchi et al. 2000), and the growth of the boundary layer above the forest. Open-canopy forests tend to be better coupled to the atmosphere than closed-canopy forests as a result of differences in climate and conductance of water vapor (Jarvis 1985). Micrometeorological studies have shown that high leaf area indices (LAI) limit turbulence, reduce wind and decrease aerodynamic conductance (Meyers et al. 1989). Pereira and Shaw (1980) showed that roughness length and zero plane displacement decrease with increasing LAI. Soil processes are also influenced by greater penetration of solar energy through the canopy (Ritchie et al. 1972, Shuttleworth 1988).

Many canopy and ecosystem models require knowledge of light interception by foliage for simulating photosynthetic carbon uptake and net ecosystem exchange (NEE) of carbon and water vapor (transpiration and evaporation) in response to climatic and nutritional conditions (Ågren et al. 1991). The LAI, defined here as half total leaf area per unit ground surface area, is generally required to parameterize models because the more leaves that intercept light, the greater the potential for carbon assimilation and water vapor transfer. A complication arises, however, because of the nonlinearity of these processes.

Terrestrial vegetation in the western USA commonly grows in water-limited conditions, resulting in landscapes with widely spaced plants and low leaf areas. These factors raise the question of the appropriateness of determining leaf area from optical measurements through inversion of radiative transfer models that assume a uniform canopy (Jarvis and Leverenz 1983). Effective leaf area (L_e), determined by one-dimensional (1-D) inversion, includes effects of branches and stems on light interception (Gower and Norman 1991). Various methods have been developed to correct optical measurements for clumping and light interception by branches and stems (Stenberg 1996, Chen et al. 1997, Gower et al. 1998).

The finer details of canopy architecture required for a complete analysis of radiative transfer are generally not used in

broad-scale applications because of limited data and the necessity for simplifying assumptions. Nonetheless, multi-layered stands and open canopies require more detailed information on the spatial distribution of leaf area than stands with a simple architecture (Williams et al. 1996). To take account of all the ramifications of variation in canopy architecture, three-dimensional (3-D) radiative models have been developed (Norman and Welles 1983, Cescatti 1997*a*). These models require an accurate description of the canopy architecture in terms of tree position, crown shapes and the amount and spatial distribution of leaf area in the single crown envelopes. One approach is to use a 3-D model to parameterize a 1-D process model by "spreading" the more realistic leaf area estimate across the landscape.

For several years, we have conducted eddy covariance and ecological measurements of carbon and water vapor exchange in a ponderosa pine (*Pinus ponderosa* Dougl. *ex* Laws.) forest in east-central Oregon (Law et al. 1999*a*). These forests have relatively discontinuous canopies with low leaf areas, and experience drought during the summer. In this study, we first obtained optical and canopy geometry measurements, then applied a 3-D model (Cescatti 1997*a*) to compare the implications of various simplifying assumptions: homogeneous or discontinuous canopies, and the effect of needle and shoot clumping. From the analysis, we sought possible simplifications applicable with the 1-D, multi-layer model, CANVEG (Baldocchi 1997). This allowed us to investigate the influences of clumping and leaf area index on estimates of carbon, water and energy exchange in the ponderosa pine forest.

Materials and methods

Site description

Most measurements were made during the summer of 1997 in a ponderosa pine (*Pinus ponderosa*) forest located in a Research Natural Area in the Metolius River basin (44°30′ N, 121°37′ W, elevation 940 m, 1% slope) east of the Cascade Mountains in Oregon. The forest grows in a region subject to warm dry summers and cold wet winters. Based on data from 45 plots (8-m radius), about 48% of the area is mixed young and old trees, 27% is open stands of old trees (~250 years old, 34 m in height), and 25% is denser patches of younger trees (~45 years old, 10 m in height; Law et al. 1999*a*). Mean characteristics of trees on the study plot are shown in Table 1.

Ponderosa pine needles are long (18 to 20 cm), three per fascicle, and clustered at the outer 20 to 50 cm of shoots. At our research site foliage is retained for 3 to 4 years. Older trees are free of branches on the lower two-thirds of the stems, and have crowns that are conical or almost flat-topped. In 1996 and 1997, bud break occurred in mid-May, and full needle expansion occured in mid-August during the summer drought. Mean tree spacing across the site is 10 m. The understory is sparse with patches of bitterbrush (*Purshia tridentata* (Pursh) DC) and bracken fern (*Pteridium aquilinum* (L.) Kuhn), and groundcover of strawberry (*Fragaria vesca* L.).

Table 1. Means and standard errors (in parenthesis) of estimates for the 100 × 100-m plot.

Variable	Young	Old
Trees ha^{-1}	553	45
Tree height (m)	10 (0.2)	34 (0.8)
Mean crown depth (m)	5 (0.1)	24 (1.3)
Mean crown ratio	0.52	0.70
Mean stem diameter at 1.4 m (cm)	11 (0.2)	69 (3)
Mean crown radius (m)	1.5 (0.1)	5 (0.3)
Mean SLA ($cm^2\ g^{-1}$)[1]	36.8 (0.7)	38.7 (1.5)

[1] Specific leaf area (SLA) was calculated as half total needle surface area (sampled in May).

Flux measurements

We used the eddy covariance method to make continuous flux measurements on a tower 14-m above the canopy and 2-m above ground to determine half-hourly sensible and latent heat fluxes (λE, evaporation from surfaces and transpiration), and CO_2 fluxes in 1996 and 1997. Details on the instrumentation, flux corrections and calculations were reported by Law et al. (1999*a*, 1999*b*) and Anthoni et al. (1999).

Optical measurements

A 100 × 100-m^2 plot was established about 100 m from the eddy flux tower. Optical measurements were made with an LAI-2000 (Li-Cor, Lincoln, NE) in September after full needle expansion under diffuse light at 5-m grid points. The LAI-2000 was held above the operator's head. We did not use a view restrictor. A second LAI-2000 was located as a reference on top of the flux tower above the canopy. The instruments were synchronized and calibrated to one another before the measurements.

Photosynthetically active radiation and net radiation were measured 1.5 m above ground with a quantum sensor (Li-Cor Model LI-190S) and a net radiometer (Model 6, REBS, Seattle, WA) mounted on an automated tram system that traversed 36 m horizontally. Measurements were recorded every millimeter. The tram traveled east and west over the northern portion of the 10,000-m^2 plot. Measurements were made from Days 189 to 205 in July 1996.

Tree dimension measurements

For each tree on a 70 × 100-m^2 plot nested within the 10,000-m^2 plot, we measured tree location (x and y coordinates) and diameter at breast height (DBH at 1.4 m). For trees with a DBH greater than 7 cm, we measured total height, height to the base of live crown, and height and radius of the widest portion of the crown in two to four directions. The locations of plot corners and the tram were measured with a global positioning system (Trimble Navigation Limited, Sunnyvale, CA), and differentially corrected with data from the base station at Portland, OR.

Needle clumping measurements

To estimate clumping of needles within shoots, we measured needle surface area and shoot silhouette area of 10 shoots obtained from the mid-canopy of five young and five old trees in September 1997. In May 1999, we collected shoots from the lower, mid- and upper canopy on one old and one young tree. For the September data, we measured shoot silhouette area (A_p) with a video camera-computer system (AgVision, Decagon Devices, Inc., Pullman, WA), with the shoot held horizontally, rotating the shoot for three projections (0, 45 and 90°; Chen 1996). For the May data, we used a Nikon camera (Nikon Corp., Tokyo, Japan) with a 400-mm lens and black and white slide film, and rotated the shoot on a tripod mount for three projections and four azimuths (0, 30, 60, 90), with back-lighting from a light table. Projections were repeated with a black ball of known dimensions for calibrating shoot silhouette area in image processing. The image processing to determine silhouette area was performed in Adobe Photoshop (Version 5.0, Adobe Systems, Inc., San Jose, CA) and ImageTool (Version 2.0, University of Texas Health Science Center, San Antonio, TX).

Total surface area of the needles on a shoot was determined from the product of specific leaf area (SLA = cm^2 total needle surface area g^{-1} dry weight) of a subsample of needles in each age class and the mass of needles, in each age class.

LAI from 1-D model inversion

The below- and above-canopy LAI-2000 measurements were merged using the Li-Cor LAI-2000 program (c2000.exe) to calculate effective LAI. All five rings were used in the calculations. The LAI-2000 software is based on the inversion of a 1-D model of light interception, and provides an estimate of effective leaf area (L_e).

LAI corrected for clumping and wood interception

The LAI-2000 measurements were corrected for clumping and interception of incident light by supporting branches and stems as described by Chen (1996):

$$L_{hc} = (1-\alpha)L_e\gamma_E/\Omega_E, \quad (1)$$

where L_{hc} is half-total surface area per m^2 ground corrected for clumping at the needle and shoot scales and wood interception; γ_E is needle-to-shoot area ratio for foliage clumping within the shoot; Ω_E is element clumping index that quantifies the effect of foliage clumping at scales larger than the shoot; and α is woody-to-total area ratio ($\alpha = W / (L_e \gamma_E/\Omega_E)$), where W is wood surface area index (half-total wood surface area m^{-2} ground, including branches (B) and stems (S)). This approach assumes that woody materials have a spatial distribution similar to foliage, and may result in a small error in the LAI estimates (Chen et al. 1998).

To determine stem area for W, we used the 7,000-m^2 plot measurements of tree diameter and height, and a taper equation developed at the site (Steve Garmon, Oregon State University, Corvallis, OR; unpublished data). For each tree, we calculated half-surface area of a cylinder from the ground to dbh, the frustum of a cone for four segments of equal height, and a cone for the treetop (sixth segment). We also used the FOREST model and tree dimension data from the 7,000-m^2 plot to calculate half-stem area per unit ground area. For branch area, we used an allometric equation developed at a nearby ponderosa pine site to estimate branch biomass per m^2 ground (Gholz 1982), and our site measurements of sapwood density of wood cores (0.407 g cm^{-3}) to calculate branch volume per m^2 ground. This was converted to half-branch area from the mean branch radius in the two diameter classes (0–30 cm, > 30 cm).

We determined Ω_E by inversion of the 3-D model. The needle-to-shoot area ratio was calculated from:

$$\gamma_E = A_{tn}/4\overline{A}_p, \quad (2)$$

where A_{tn} is total needle surface area on a shoot, and $\overline{A}_p$ is mean projected shoot silhouette area (Stenberg 1996).

Leaf area, canopy architecture, and radiation regime from 3-D modeling

Spatially explicit LAI-2000 measurements were coupled with a 3-D canopy model (FOREST; Cescatti 1997*a*) that reproduces stand geometry by accounting for position and crown shape of single trees on the plot. The crown model allows the description of highly asymmetric crown shapes and of bending trees as they typically appear in natural forests. The crown of each tree was stratified into three nested layers that present different densities of branch and leaf area. The probabilities of penetration of direct and diffuse radiation were modeled separately with a Markov model (Nilson 1971). Diffuse radiation resulting from scattering was estimated by the adding method (Norman and Jarvis 1975).

Given the coordinates of the sampling points, the model generates a hemispherical view of the canopy as seen from the LAI-2000 (Cescatti 1997*b*), and assuming a certain value of leaf area density (LAD) in the crowns, it predicts canopy transmittance for the five rings of the LAI-2000 sensor. To avoid the edge effect, only the LAI-2000 sampling points well within the experimental plot were used in the inversion. Furthermore, only the values of canopy transmittance in the three intermediate rings (2, 3 and 4) were used. The inner LAI-2000 ring (1) was excluded because measurements by this ring are too sensitive to the sensor position with respect to the crown projections and are therefore affected by errors in the description of the stand geometry. The external ring (5) was excluded because measurements of canopy transmittance in this ring are significantly increased by scattered radiation.

Leaf area was estimated by changing the LAD in the crown layers iteratively to minimize the square error between the model prediction and the LAI-2000-measured transmittance according to the Quasi-Newton algorithm. The value of LAD that minimized the sum of square errors was used to calculate leaf area of each tree and the stand. This estimate of leaf area is already corrected for the effect of leaf clumping at the crown

level and stem area. We applied γ_E and B to obtain the final estimate of leaf area ($L_{3\text{-D}}$), which was used as input to the CANVEG model (Figure 1):

$$L_{3\text{-D}} = (L_e - B)\gamma_E. \quad (3)$$

Stand architecture was modeled based on two assumptions about canopy heterogeneity in horizontal space: (1) that the canopy is homogeneous horizontally and has a stand average vertical profile; and (2) that the canopy is heterogeneous based on crown envelopes at the observed spatial location. The effect of different canopy architectures on the radiative regime was evaluated separately for direct (D) and diffuse (d) radiative fields.

The probability of non-interception of beam radiation passing through a canopy was computed in the model with the Beer-Lambert equation and the beam paths in the crown array (Nilson 1992). The beam path length and the LAD along the path in each crown were computed with an angular resolution of 1° for the upper hemisphere (360° by 90° directions). A complete description and validation of the light interception model is reported in Cescatti (1997*a*, 1997*b*).

The 3-D model of the canopy was used to describe the radiative regime of the forest during the growing season (Days 135–287). Half-hourly values of global and PAR radiation measured above the canopy in 1996 were used as input fluxes. The model computed canopy transmittance to D and d separately, with a time step of 0.01 h for the growing season at each node of a 3-D grid (31 nodes north, 46 east, 25 altitude) of 35,650 points with 2-m spacing. The mean and standard deviation of transmittance at the 25 heights were computed separately for the nodes inside and outside the tree crowns.

Mass and energy transfer modeling

The CANVEG model is a 1-D, multi-layer biosphere–atmosphere gas exchange model that has coupled micrometeorological and physiological modules (Baldocchi 1997). The micrometeorological model computes leaf and soil energy exchange, turbulent transfer, carbon and water vapor profiles and radiative transfer through the canopy. The radiative transfer computations provide probabilities of sunlit and shaded leaves for calculations of photosynthesis, leaf energy balance, and turbulent transfer of CO_2, water vapor and sensible heat.

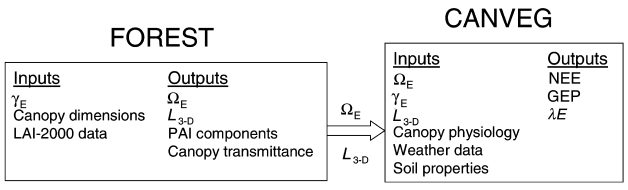

Figure 1. Schematic of FOREST and CANVEG model inputs and outputs, and linkage through FOREST estimates of effective leaf area ($L_{3\text{-D}}$) and clumping index at scales larger than shoots (Ω_E). Abbreviations: γ_E = needle-to-shoot area ratio for clumping within shoot; λE = ecosystem water vapor exchange; NEE = net ecosystem exchange; and GEP = gross ecosystem productivity.

The physiological module computes leaf photosynthesis, stomatal conductance, transpiration, respiration by foliage and woody tissue, and soil CO_2 flux (respiration by roots and microbes). Stomatal conductance was calculated as a function of assimilation, relative humidity and CO_2 concentration at the leaf surface (Collatz et al. 1991). The CO_2 and water vapor diffusive source strength are modeled from LAD with respect to height, concentration difference between the air outside the laminar boundary layer of leaves and within stomata, boundary layer resistance to molecular diffusion, stomatal resistance and air density. The change in concentration summed over the canopy layers is combined with soil fluxes to estimate whole-ecosystem CO_2 and λE fluxes. Details of model computations are described in Baldocchi (1997), model inputs are shown in Table 2, and a schematic of the linkage between FOREST and CANVEG is shown in Figure 1.

The clumping corrections appear in several computations in the radiative transfer module, including a Markov model (Myneni et al. 1989) for the probability of diffuse and direct beam penetration, and layer transmission and reflectance computations. We evaluated the effect of assuming random distribution of foliage on mass and energy transfer by running the model with and without clumping corrections (γ_E and Ω_E together and independently), and compared model estimates of NEE of CO_2 and water vapor. To evaluate the differences in NEE that may be associated with assumptions of horizontal homogeneity, we ran CANVEG with leaf area values from the frequency distribution computed from FOREST.

Results and discussion

Micrometeorological observations

Tram measurements of PAR transmittance (Q_p) to the forest floor in the ponderosa pine forest showed a heterogeneous light environment. Within the ponderosa pine stand, sun patches exceeded 5 m in length and the energy within the sun patches exceeded that in shade patches by more than 1000 μmol m^{-2} s^{-1} (Figure 2a). In contrast, the dimension of typical sunflecks in a boreal jack pine stand was generally less than 1m (Baldocchi et al. 2000). The fraction of transmitted PAR ($Q_p(0)/Q_p(h)$, where $Q_p(0)$ is PAR transmittance below canopy measured at 1.5 m above ground, and $Q_p(h)$ is incident PAR above canopy), was greater and more variable diurnally in the more open ponderosa pine forest compared with jack pine and a closed-canopy temperate deciduous forest (Figure 2b).

The openness of forest canopies has a large effect on the energy budget. The proportion of net radiation measured at the forest floor ($R_n(0)$) of the ponderosa pine forest, compared with measurements above the canopy ($R_n(h)$), varied slightly from 31% in May to 25% in August 1997. There was more variation in a boreal jack pine forest (LAI ~2.0), where the proportion ranged from 10 to 30% (Baldocchi et al. 1998). In contrast, < 8% of available net radiation was received at the forest floor of a closed-canopy temperate deciduous forest with an LAI of ~5.0 (Hutchison and Baldocchi 1989) (Fig-

Table 2. Key parameters for the CANVEG model.

Description	Value	Reference
Latitude	44°29′ N	Law et al. 1999*a*
Longitude	121°37′ W	Law et al. 1999*a*
Maximum LAI (m^2 projected m^{-2} ground)	1.6	FOREST model
Canopy height (m)	34	Law et al. 1999*a*
V_{cmax} at 25 °C (μmol m^{-2} s^{-1})	73	Law et al. 2000*b*, Middleton et al. 1998, Sullivan et al. 1997
J_{max} (μmol m^{-2} s^{-1})	170	Middleton et al. 1998, Sullivan et al. 1997
Ball-Berry constant, *k*	8.0	Harley and Baldocchi 1995
Apparent quantum yield (mol CO_2 (mol quanta)$^{-1}$)	0.04	Law et al. 1999*b*
Element clumping index at scales larger than shoot, Ω_E	0.83	FOREST model or tram data
Needle-to-shoot area ratio for needle clumping within shoot, γ_E	1.29	This study
Soil surface CO_2 flux at 25 °C (μmol m^{-2} s^{-1})	3.9	Law et al. 1999*b*
Q_{10} for foliage respiration	2.0	Harley and Baldocchi 1995
Q_{10} for sapwood respiration	2.02	Harley and Baldocchi 1995
Base temperature for photosynthesis, T_b (K)	311	Collatz et al. 1991
Activation energy, E_a for CO_2 (J mol^{-1})	65,120	Lloyd and Taylor 1994
Soil resistance to evaporation (s m^{-1})	816	Camillo and Gurney 1986

ure 3). In the ponderosa pine forest, vapor pressure deficit (VPD) measured at 1 m height averaged only 0.1 kPa less than that measured above the canopy, indicating the sub-canopy environment was closely coupled with the atmosphere (Jarvis 1986). Soil temperature (2-cm depth) often exceeded above-canopy (45 m) air temperature (by 1.6 °C from May to October). Large amounts of radiation received at the forest floor have implications for respiration and NEE, because soil surface CO_2 efflux increases with temperature (Lloyd and Taylor 1994, Law et al. 1999*a*, 1999*b*).

Previously, Law et al. (2000*a*) showed that the ratio of gross ecosystem productivity (GEP) to transpiration, estimated from the combination of chamber and tower flux data, decreased with increasing VPD. Leaf-level studies have shown how *A*/*E* (assimilation to transpiration) decreased with VPD and temperature, and suggested that variation in the ratio can also be explained by the high degree of coupling of the vegetation and soil surface to the atmosphere (e.g., Jarvis 1986). Clearly, the degree of openness of the canopy affects this ratio.

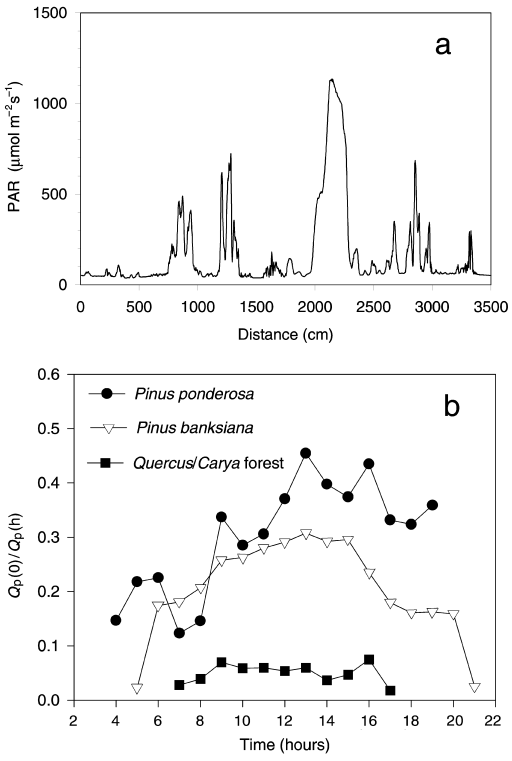

Figure 2. (a) Horizontal distribution of transmitted PAR (Q_p) measured by the 36-m long tram in the ponderosa pine forest in July 1996 (Day 188), between 0810 and 0853 h (PST). Mean Q_p was 169 μmol m^{-2} s^{-1} (SD = 230 μmol m^{-2} s^{-1}). (b) Fraction of incident PAR transmitted below the canopy ($Q_p(0)/Q_p(h)$) in three forests. Note the large diurnal variation in the more open *P. ponderosa* canopy that includes a large range of tree sizes (data sources: *Pinus banksiana*, Baldocchi et al. 1998; *Quercus–Carya* forest, Hutchison and Baldocchi 1989).

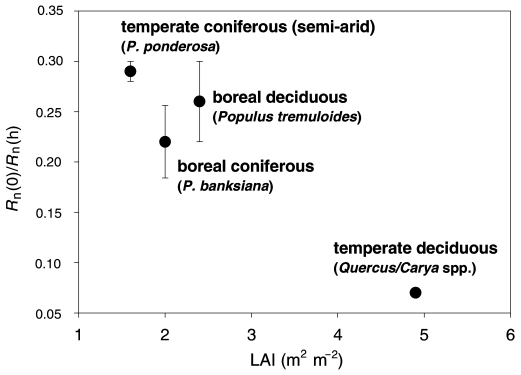

Figure 3. Ratio of net radiation measured at the forest floor ($R_n(0)$) to net radiation measured above the canopy ($R_n(h)$) in relation to leaf area index (summer maximum LAI, m^2 half surface area m^{-2} ground) of different forest types, including our site (*P. ponderosa*), boreal jack pine (*P. banksiana*; Baldocchi et al. 1998), boreal aspen (*P. tremuloides*; Black et al. 1996) and a temperate deciduous forest (*Quercus* and *Carya* spp.; Hutchison and Baldocchi 1989).

As leaf area decreases, significant radiation flux reaches the forest floor, with the result that a substantial portion of λE is derived from the understory and soils. Forest floor λE ranged from 0.4 to 0.7 mm day^{-1} through the year. The proportion of total latent heat flux (λE) derived from the forest floor ranged from 22% in July to 55% in March, with higher proportions in the wet season than in the dry season (Figure 4). Compared with forests with different maximum LAI, the proportion of total λE derived from the forest floor increased as leaf area became more sparse (Figure 5), and appeared to change little above LAI > 3 (Hutchison and Baldocchi 1989, Kelliher et al. 1990, Lafleur et al. 1993, Baldocchi et al. 1998). Figure 5 shows the modeled relationship for ponderosa pine using CANVEG, which also indicates an increase in the proportion of total λE from the forest floor with decreasing LAI. Although $\lambda E(0)/\lambda E(h)$ – LAI is not a functional relationship, it is useful to demonstrate that it can be inappropriate to model evaporation as a constant fraction of precipitation or total λE through the year. Annual total λE at our site was 436 ± 65 mm in 1996 and 400 ± 60 mm in 1997, and soil evaporation was ~38% of precipitation in both years, as determined from above- and below-canopy λE measurements. In a previous modeling exercise, evaporation from the canopy and soil surface was assumed to be 15% of precipitation (Law et al. 2000*a*), which, combined with other factors (e.g., one-layer soil model), resulted in substantial underestimation of evaporation. A correlation such as that shown in Figure 5, enveloping evaporation in wet and dry conditions, could be used to scale soil evaporation or transpiration fractions of total λE with maximum leaf area in such models.

Leaf area and clumping estimates

Figure 6 illustrates the probability density function of point estimates of L_e on the 10,000-m^2 plot calculated from the LAI-2000 1-D model. The plot mean L_e was 1.3 ± 0.1. The measurements of L_e were corrected for the needle-to-shoot ratio for needle clumping within the shoot (γ_E), the element clumping index at scales larger than shoot (Ω_E), and woody surface area index (W; Equations 1 and 2). Figure 7 shows the shoot silhouettes for three shoot angles at 0 azimuth. The mean γ_E was similar seasonally; 1.29 ± 0.04 in September 1997 and 1.25 ± 0.10 in May 1999 (Table 3). Higher values of γ_E indicate more needle clumping. Seasonal change in needle biomass per shoot was 25%, and changes in needle and shoot area were 27 and 21%, respectively, lending support to the concept that γ_E increases with a greater change in needle area than silhouette area as new needles elongate. Chen et al. (1997) calculated γ_E of 1.2 to 1.5 for young and old boreal jack pine (*Pinus banksiana* Lamb.) and found a comparable seasonal increase in γ_E from early to late summer as needle area within shoots increased more than shoot area. Values of γ_E for red pine (*Pinus resinosa* Ait.), which has slightly shorter needles than other pine species, ranged from 1.6 (Deblond et al. 1994, corrected for half-surface area) to 2.1 (Chen and Cihlar 1995). Stenberg (1996) observed a range of γ_E between 1.25 and 2.5 for Scots pine (*Pinus sylvestris* L.), which has short, clustered needles. Studies have shown that sun-acclimated shoots have a larger γ_E than shaded shoots, and pines in general have larger maximum γ_E than other conifer species (Leverenz and Hinckley

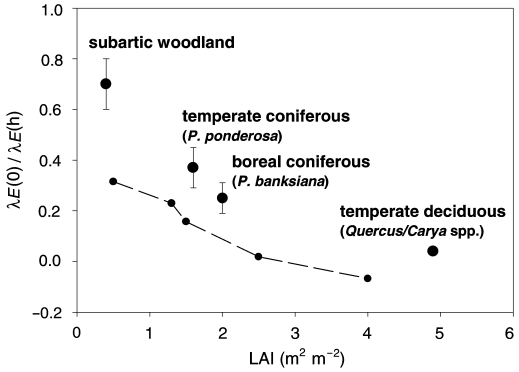

Figure 5. Proportion of total latent heat flux (λE(h)) observed at the forest floor (λE(0)) increases as leaf area (summer maximum LAI, m^2 half surface area m^{-2} ground) becomes more sparse. The dashed line is $\lambda E(0)/\lambda E$(h) computed for different LAI values using the CANVEG model (including clumping factors).

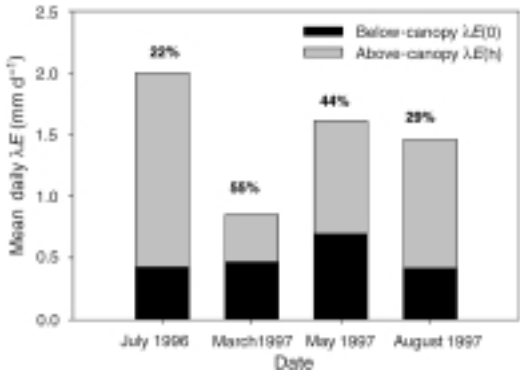

Figure 4. Proportion of total latent heat flux (λE(h)) derived from the forest floor (λE(0)) in the ponderosa pine forest was greatest during the wet season (March and May).

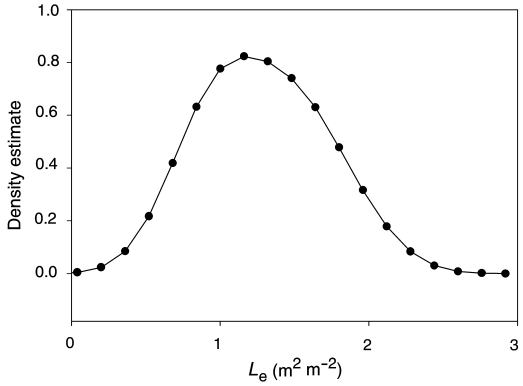

Figure 6. Probability density function of 242 LAI-2000 1-D inversion estimates of effective leaf area (L_e, m^2 half surface area m^{-2} ground) on the 10,000-m^2 plot.

Figure 7. The silhouette of a ponderosa pine shoot at azimuth 0 and shoot angles of 0, 45 and 90°.

1990, Stenberg et al. 1995, Leverenz 1996, Sprugel et al. 1996, Stenberg 1996). At our site, the younger (45-year-old) trees are shaded more frequently than the old-growth trees. Leaf mass per unit area, foliar N/area, and γ_E decreased by 5, 18, and 24%, respectively, from the upper to lower canopy of the young trees, as expected in closed-canopy forests (Reich et al. 1997). The reverse was true for the old trees, with the highest values in the lower canopy. We found that the mean γ_E from mid-canopy of the young trees was 1.22 (SE 0.04), and 1.36 (SE 0.04) for the old-growth trees at full leaf.

The Ω_E generally ranges from 0.65 to 1.0, with higher values indicating less canopy clumping. The Ω_E for a given site can change by as much as 20% with a 40° change in solar zenith angle (Chen 1996). Most reported values are within 0.1 of 0.75 (Chen et al. 1998). Inversion of the 3-D model yielded a Ω_E of 0.83 integrated over all solar zenith angles observed in summer (Table 3). We obtained the same results (Ω_E at 1 radian = 0.83) from gap analysis of the PAR data collected by the tram. We observed less clumping than in a mature jack pine stand in summer (0.75; Chen et al. 1998), and more clumping than in a 60-year-old red pine plantation (0.91; Chen and Cihlar 1995).

Half-stem surface area per unit ground area (S) from the FOREST model for the 7,000-m^2 plot was 0.23, and the estimate from simple modeling of the stem sections was 0.21. Woody surface area index (W) was 0.33 m^2 half-total wood area per m^2 ground using the FOREST model estimate of S and our biomass estimate of half-branch area (B = 0.10). The value of $1 - \alpha$ from Equation 1 was 0.84 based on the L_e determined by the LAI-2000 and the 3-D model estimate of Ω_E. This is similar to the values Chen et al. (1998) obtained for old black spruce (*Picea mariana* (Mill); 0.71) and young jack pine (*Pinus banksiana*; 0.72 to 0.95). Table 3 summarizes the leaf area and clumping estimates. The L_{hc} was 1.69 using Equation 1, which assumes that wood is clumped in the same manner as foliage and likely results in an overestimate of leaf area.

Table 3. Leaf area (m^2 half surface area m^{-2} ground) estimated by different methods. Effective leaf area (L_e) was calculated from LAI-2000 measurements and a 1-D inversion model (LAI-2000 software). Variable Ω_E, calculated from the FOREST model, is the clumping index for scales larger than shoot. Variable γ_E is the needle-to-shoot area ratio for needle clumping within the shoot (Equation 2), and L_{hc} is calculated from Equation 1. The 3-D FOREST model estimate ($L_{3\text{-}D}$) was calculated from Equation 3.

Variable	Leaf area	*n*
W	0.33	–
$1 - \alpha$	0.84	–
Ω_E	0.83	–
γ_E (minimum leaf)	1.25 (0.10)	6
γ_E (maximum leaf)	1.29 (0.04)	10
L_e	1.3 (0.1)	242
L_{hc}	1.7	242
$L_{3\text{-}D}$	1.6 (0.01)	28,000

Leaf area and canopy architecture from 3-D model

The tree locations, canopy dimensions, and LAI-2000 sample locations used to compute radiative transfer and LAI with the 3-D model are shown in Figure 8. The 3-D model explained 62% of the variance in the spatial distribution of canopy transmittance. The LAD that minimized the square error between observed and predicted transmittances in the external, intermediate and inner crown layer were 0.36, 0.08 and 0.03 m^2 m^{-3}, respectively. The surface area of single trees in the experimental plot was calculated from the product of LAD and vol-

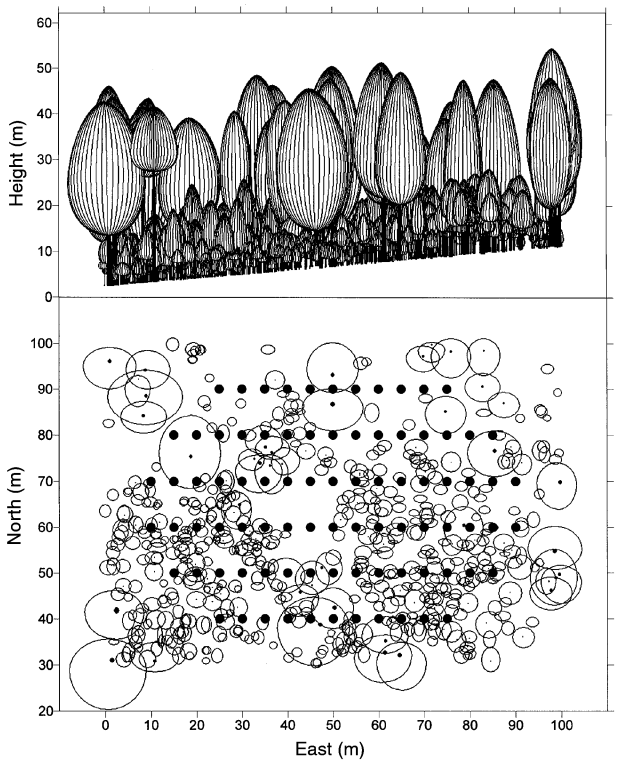

Figure 8. Spatially explicit LAI-2000 measurements and measurements of canopy dimensions were used in a 3-D canopy model to reproduce stand geometry by accounting for position and crown shape of single trees on the plot. The solid circles indicate locations of LAI-2000 measurements that were well within the plot for the model inversion estimate of LAI.

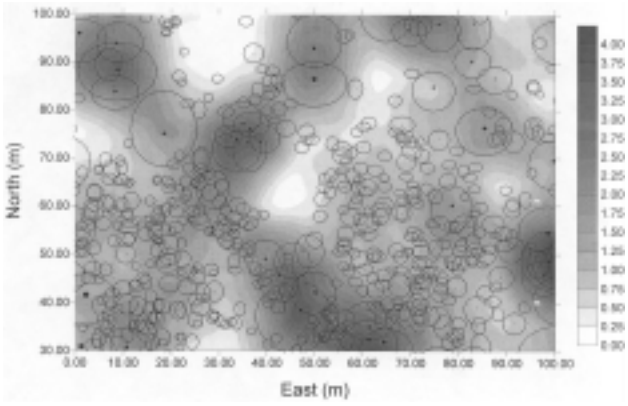

Figure 9. Values of $L_{3\text{-D}}$ computed by the 3-D model for each of 28,000 circular plots (8-m radius) spaced 0.5 m apart in a grid covering the 10,000-m^2 plot. The $L_{3\text{-D}}$ value at the center of each circular plot is shown in gray tones.

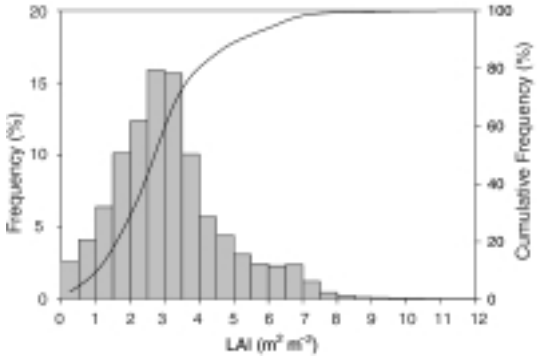

Figure 10. Frequency distribution $L_{3\text{-D}}$ from the 3-D modeling for 28,000 subplots within the 10,000-m^2 plot. Mean $L_{3\text{-D}}$ = 1.6 (SD = 0.81).

ume of each crown layer. Using the γ_E of 1.29 in Equation 3, mean $L_{3\text{-D}}$ was 1.63, 23% higher than L_e. Half of the total plant area index (PAI), which includes foliage and woody material, was calculated as PAI = $L_{3\text{-D}} + B + S = 1.63 + 0.10 + 0.23 = 2.0$.

To evaluate canopy heterogeneity, $L_{3\text{-D}}$ was computed for each of 28,000 circular plots (8-m radius) spaced 0.5 m apart in a grid covering the 10,000-m^2 plot. The $L_{3\text{-D}}$ value at the center of each circular plot is shown in gray tones in Figure 9, and the frequency distribution of $L_{3\text{-D}}$ in the 28,000 subplots is reported in Figure 10. Values of $L_{3\text{-D}}$ ranged from 0 to 5 with an average of 1.6 (SD = 0.81) and a skewed distribution.

Based on the estimated surface area density in each crown layer and the vertical distribution of crown volumes, the vertical distribution of the different components of PAI (stems, branches and needles) was computed. Figure 11 shows the bimodal vertical distribution of surface area due to the multi-layered structure of the forest with two major layers of overstory and understory trees (Figure 8). Vertical distribution data are useful for multi-layer canopy gas exchange models (e.g., Law et al. 2000*b*).

Characterization of the radiative regime by 3-D model

Figure 11 shows the mean vertical profile of canopy transmittance predicted by a 1-D model compared with the profile determined by the 3-D model. Results show that the penetration of radiative fluxes was greater when modeled in 3-D than in 1-D because of leaf clumping in crowns. The increase in PAR transmittance to the forest floor was 8% in direct radiation (39% at the forest floor from the 3-D model versus 31% from the 1-D model) and 5% in the diffuse flux (28% versus 23%). This is likely to be a function of leaf area, in that 1-D and 3-D model estimates of transmittance may converge at low and high leaf areas, and diverge at mid-range values. These are questions that can be addressed with sensitivity analyses.

Mean vertical profiles of light penetration in heterogeneous canopies do not offer a comprehensive view of the radiative regime. A quantitative estimation of the spatial variability in the radiative field is shown in Figure 12, where means and standard deviations of canopy transmittance in the 7,000-m^2 plot are presented separately for the space inside and outside of crowns. The large spatial variability in the direct radiation within the crown space of both the dominant and suppressed trees could affect the leaf and soil energy balance, and thus CO_2 exchange of the canopy.

Mass and energy transfer modeling

The CANVEG model can simulate feedbacks between leaf temperature, energy balance, stomatal conductance and pho-

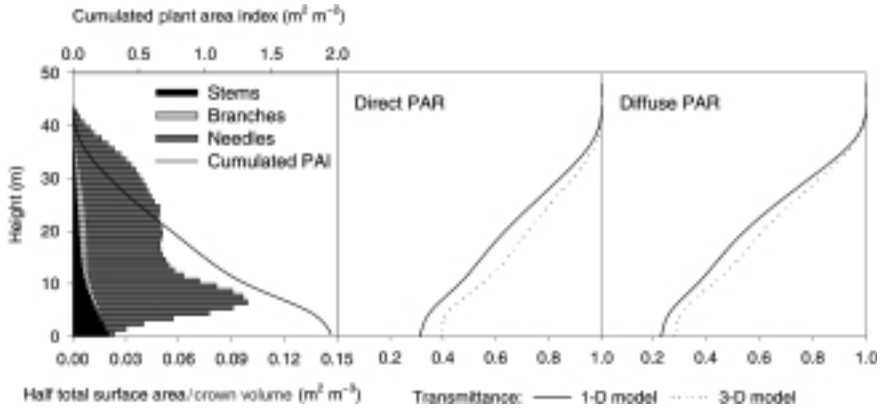

Figure 11. Vertical distribution of plant area index (PAI), and components of PAI, showing the bimodal vertical distribution attributable to the multi-layered structure of the forest. The vertical profile of the mean canopy transmittance of direct and diffuse radiation predicted by a 1-D model is compared with that from the 3-D model. The penetration of radiative fluxes was greater when modeled in 3-D, showing that the 1-D model underestimated direct and diffuse transmittance by 8 and 5%, respectively.

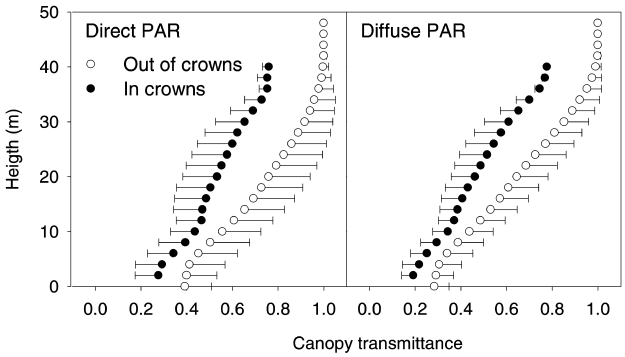

Figure 12. Spatial variation in canopy transmittance from the 3-D model, showing means and standard deviations in the 7,000-m^2 plot for the space inside and outside of crowns. Note the large spatial variation in direct radiation within the crown space.

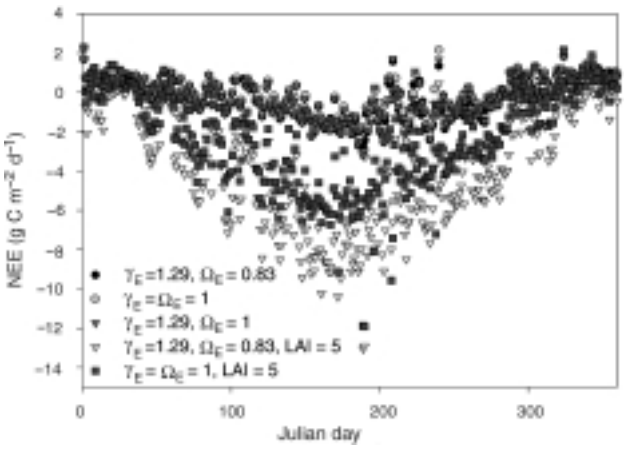

Figure 13. Mean daily net ecosystem exchange (NEE) estimated from CANVEG, based on assuming random distribution of foliage (γ_E = Ω_E = 1), clumping at all scales (γ_E = 1.29, Ω_E = 0.83), and various combinations at measured LAI and at LAI 5. Negative NEE values indicate more net carbon uptake by vegetation. The NEE was affected more than any other variable, and net photosynthesis was affected more at higher leaf areas.

tosynthesis, which are likely to be perturbed with variation in LAI. We evaluated the impact of clumping on annual fluxes of carbon dioxide and water (Table 4). Assuming random distribution of foliage (γ_E = Ω_E = 1) in CANVEG resulted in annual λE that was only slightly lower (10%) than when clumping factors (γ_E = 1.29, Ω_E = 0.83) were included; however, soil evaporation was underestimated by 40% when clumping factors were excluded. A random distribution assumption also resulted in a net carbon uptake that was 41% lower than when clumping factors were included (Figure 13, Table 4), net photosynthesis was lower by 3%, and total λE was lower by 10%. The same comparisons at a hypothetical LAI of 5 showed a similar effect of reduced values on annual NEE estimates (37%) and λE (12%), but a larger effect on net photosynthesis (20%), possibly because of substantial changes in sunlit and shaded fractions of foliage at the higher leaf area when clumping is assumed. The effect on annual NEE of including γ_E alone or Ω_E alone was similar (59 and 54%, respectively) compared with annual NEE when random distribution was assumed, so clearly all scales of clumping need to be addressed in simulating processes of this forest. Our past work, in a closed-canopy deciduous forest showed that clumping had a marked impact on canopy photosynthesis (Baldocchi and Harley 1995). Work on the sparser ponderosa pine stand has demonstrated that the impact of clumping on photosynthesis diminishes as leaf area decreases, even though the clumping in crowns is great. This finding has implications for the application of biogeochemical models that ignore leaf clumping and its effects on light transfer and photosynthesis. The errors are smaller than one would have surmised working only with broad-leaved canopies. Such a finding emphasizes the importance of working across a spectrum of forest types.

Further work is required to determine how 3-D predictions of foliage distribution may be simplified for 1-D modeling of CO_2 and water vapor exchange. In the meantime, a combination of micrometeorological and ecological measurements will allow us to continue to evaluate responses of open-canopied forests to environmental factors at multiple scales.

Acknowledgments

This study was funded by NASA (grants #NAGW-4436 and #NAG5-7551) and by the Province of Trento, Italy (DL 14616). We thank Steve Van Tuyl and Will Hutchinson for their contributions to field and laboratory measurements, and to Lisa Ganio for her statistical advice. We thank Dr. Richard Waring for constructive comments

Table 4. Estimates from CANVEG of annual net ecosystem exchange (NEE, negative value indicates net uptake by vegetation), net photosynthesis (P_n), gross ecosystem production (GEP), water vapor exchange (λE), and soil evaporation (λE_{soil}), assuming random distribution of foliage (γ_E = Ω_E = 1) versus inclusion of clumping factors (γ_E = 1.29, Ω_E = 0.83).

Hypothesis	NEE (g C m^{-2} $year^{-1}$)	P_n (g C m^{-2} $year^{-1}$)	GEP (g C m^{-2} $year^{-1}$)	λE (mm $year^{-1}$)	λE_{soil} (mm $year^{-1}$)
γ_E = 1.29, Ω_E = 0.83	–70	1117	1267	409	58
γ_E = Ω_E = 1	–41	1087	1236	367	35
γ_E = 1.29, Ω_E = 1	–65	1111	1262	385	41
γ_E = 1, Ω_E = 0.83	–63	1109	1260	377	33
LAI = 5; γ_E = 1.29, Ω_E = 0.83	–1367	2545	2903	761	–
LAI = 5; γ_E = Ω_E = 1	–855	2033	2379	666	–

on an earlier version of this manuscript, and Peter Anthoni for providing eddy flux data and advice on analysis. We gratefully acknowledge the assistance of the Sisters Ranger District of the US Forest Service in establishing the study site, which is located in a Research Natural Area—an area selected to represent vegetation types in a natural condition.

References

Ågren, G.I., R.E. McMurtrie, W.J. Parton, J.Pastor and H.H. Shugart. 1991. State-of-the-art of models of production–decomposition linkages in conifer and grassland ecosystems. Ecol. Appl. 1: 118–138.

Anthoni, P.M., B.E. Law and M.H. Unsworth. 1999. Carbon and water vapor exchange of an open-canopied ponderosa pine ecosystem. Agric. For. Meteorol. 95:151–168.

Baldocchi, D.D. 1997. Measuring and modelling carbon dioxide and water vapour exchange over a temperate broad-leaved forest during the 1995 summer drought. Plant Cell Environ. 20:1108–1122.

Baldocchi, D.D. and P.C. Harley. 1995. Scaling carbon dioxide and water vapour exchange from leaf to canopy in a deciduous forest. II. Model testing and application. Plant Cell Environ. 18: 1157–1173.

Baldocchi, D.D., C.A. Vogel, and B. Hall. 1998. Seasonal variation of energy and water vapor exchange rates above and below a boreal jack pine forest canopy. J. Geophys. Res. 102:28,939–28,952.

Baldocchi, D.D., F.M. Kelliher, T.A. Black and P.J. Jarvis. 2000. Climate and vegetation controls on boreal zone energy exchange. Global Change Biol. 6:69–83.

Black, T.A., G. den Hartog, H.H. Heumann, P.D. Blanken, P.C. Yang, C. Russell, Z. Nesic, X. Lee, S.G. Chen, R. Staebler and M.D. Novak. 1996. Annual cycles of water vapour and carbon dioxide fluxes in and above a boreal aspen forest. Global Change Biol. 2:219–229.

Camillo, P.J. and R.J. Gurney. 1986. A resistant parameter for bare-soil evaporation models. Soil Sci. 141:95–105.

Cescatti, A. 1997*a*. Modelling the radiative transfer in discontinuous canopies of asymmetric crowns. I. Model structure and algorithms. Ecol. Model. 101:263–274.

Cescatti, A. 1997*b*. Modelling the radiative transfer in discontinuous canopies of asymmetric crowns. II. Model testing and application in a Norway spruce stand. Ecol. Model. 101:275–284.

Chen, J.M. 1996. Optically-based methods for measuring seasonal variation of leaf area index in boreal conifer stands. Agric. For. Meteorol. 80:135–163.

Chen, J.M. and J. Cihlar. 1995. Plant canopy gap-size analysis theory for improving optical measurements of leaf-area index. Appl. Optics 34:6211–6222.

Chen, J.M., P.D. Blanken, T.A. Black, M. Guilbeault and S. Chen. 1997. Radiation regime and canopy architecture in a boreal aspen forest. Agric. For. Meteorol. 86:107–125.

Chen, J.M., P.M. Rich, S.T. Gower, J.M. Norman and S. Plummer. 1998. Leaf area index of boreal forests: Theory, techniques, and measurements. J. Geophys. Res. 102:29,429–29,443.

Collatz, G.J., J.T. Ball, C. Grivet and J.A. Berry. 1991. Regulation of stomatal conductance and transpiration: a physiological model of canopy processes. Agric. For. Meteorol. 54:107–136.

Deblonde, G., M. Penner and A. Royer. 1994. Measuring leaf area index with the LI-COR LAI-2000 in pine stands. Ecology 75: 1507–1511.

Gholz, H.L. 1982. Environmental limits on aboveground net primary production, leaf area, and biomass in vegetation zones of the Pacific Northwest. Ecology 63:469–481.

Gower, S.T. and J.M. Norman. 1991. Rapid estimation of leaf area index in conifer and broad-leaf plantations. Ecology 72:1896–1900.

Gower, S.T., J.G. Vogel, J.M. Norman, C.J. Kucharik, S.J. Steele and T.K. Stow. 1998. Carbon distribution and aboveground net primary production in aspen, jack pine, and black spruce stands in Saskatchewan and Manitoba, Canada. J. Geophys. Res. 102: 29,029–29,041.

Harley, P.C. and D.D. Baldocchi. 1995. Scaling carbon dioxide and water vapour exchange from leaf to canopy in a deciduous forest. I. Leaf model parametrization. Plant Cell Environ. 18:1146–1156.

Hutchison, B.A. and D.D. Baldocchi. 1989. Forest meteorology. *In* Analysis of Biogeochemical Cycling Processes in Walker Branch Watershed. Eds. D.W. Johnson and R.I. van Hook. Springer-Verlag, New York, pp 21–95.

Jarvis, P.G. 1985. Transpiration and assimilation of tree and agricultural crops: the 'omega factor.' *In* Attributes of Trees as Crop Plants. Eds. M. G. R. Cannell and J. E. Jackson. Institute of Terrestrial Ecology, U.K., pp 460–479.

Jarvis, P.G. 1986. Coupling of carbon and water interactions in forest stands. Tree Physiol. 2:347–368.

Jarvis, P.G. and J.W. Leverenz. 1983. Productivity of temperate, deciduous and evergreen forests. *In* Physiological Plan Ecology IV. Ecosystem Processes, Mineral Cycling, Productivity and Man's Influence. Eds. O.L. Lange, P.S. Nobel, C.B. Osmond and H. Ziegler. Springer-Verlag, Berlin, pp 233–280.

Kelliher, F.M., D. Whitehead, K.J. McAneney and M.J. Judd. 1990. Partitioning evapotranspiration into tree and understorey components in two young *Pinus radiata* D. Don stands. Agric. For. Meteorol. 50:211–227.

Lafleur, P.M., A.V. Renzetti and R. Bello. 1993. Seasonal changes in the radiation balance of subarctic forest and tundra. Arctic Alp. Res. 25:32–36.

Law, B.E., M.G. Ryan and P.M. Anthoni. 1999*a*. Seasonal and annual respiration of a ponderosa pine ecosystem. Global Change Biol. 5: 169–182.

Law, B.E., D.D. Baldocchi and P.M. Anthoni. 1999*b*. Below-canopy and soil CO_2 fluxes in a ponderosa pine forest. Agric. For. Meteorol. 94:13–30.

Law, B.E., R.H. Waring, P.M. Anthoni and J.D. Aber. 2000*a*. Measurements of gross and net ecosystem productivity and water vapor exchange of a *Pinus ponderosa* ecosystem, and an evaluation of two generalized models. Global Change Biol. 6:155–168.

Law, B.E., M. Williams, P.M. Anthoni, D.D. Baldocchi and M.H. Unsworth. 2000*b*. Measuring and modeling seasonal variation of carbon dioxide and water vapor exchange of a *Pinus ponderosa* forest subject to soil water deficit. Global Change Biol. 6:613–630.

Leverenz, J.W. 1996. Shade-shoot structure, photosynthetic performance in the field, and photosynthetic capacity of evergreen conifers. Tree Physiol. 16:109–114.

Leverenz, J.W. and T.M. Hinckley. 1990. Shoot structure, leaf area index and productivity of evergreen conifer stands. Tree Physiol. 6: 135–149.

Lloyd, J. and J.A. Taylor. 1994. On the temperature dependence of soil respiration. Funct. Ecol. 8:315–323.

Meyers, T.P., B.J. Huebert and B.B. Hicks. 1989. HNO_3 deposition to a deciduous forest. Boundary-Layer Meteorol. 49:395–406.

Middleton, E.M., J.H. Sullivan, B.D. Bovard, A.J. Deluca, S.S. Chan and T.A. Cannon. 1998. Seasonal variability in foliar characteristics and physiology for boreal forest species at the five Saskatchewan tower sites during the 1994 Boreal Ecosystem–Atmosphere Study. J. Geophys. Res. 102:28,831–28,844.

Myneni, R., J. Ross and G. Asrar. 1989. A review on the theory of photon transport in leaf canopies. Agric. For. Meteorol. 45:1–153.

Nilson, T. 1971. A theoretical analysis of the frequency of gaps in plant stands. Agric. Meteorol. 8:25–38.

Nilson, T. 1992. Radiative transfer in nonhomogeneous plant canopies. Adv. Bioclimatol. 1:59–88.

Norman, J.M. and P.G. Jarvis. 1975. Photosynthesis in Sitka spruce (*Picea sitchensis* (Bong.) Carr.). V. Radiation penetration theory and a test case. J. Appl. Ecol. 12:839–878.

Norman, J.M. and J.M. Welles. 1983. Radiative transfer in an array of canopies. Agron. J. 75:481–488.

Pereira, A.R. and R.H. Shaw. 1980. A numerical experiment on mean wind structure inside canopies of vegetation. Agric. For. Meteorol. 22:303–318.

Reich, P.B., M.B. Walters and D.S. Ellsworth. 1997. From tropics to tundra: global convergence in plant functioning. Proc. Nat. Acad. Sci. 94:13,730–13,734.

Ritchie, J.T., E. Burnett and R.C. Henderson. 1972. Dryland evaporative flux in a subhumid climate. III. Soil water influence. Agron. J. 64:168–173.

Shuttleworth, W.J. 1988. Evaporation from Amazonian rainforest. Proc. Royal Soc. London, Series B. 233:321–346.

Sprugel, D.G., J.R. Brooks and T.M. Hinckley. 1996. Effects of light on shoot geometry and needle morphology in *Abies amabilis*. Tree Physiol. 16:91–98.

Stenberg, P. 1996. Correcting LAI-2000 estimates for the clumping of needles in shoots of conifers. Agric. For. Meteorol. 79:1–8.

Stenberg, P., E.H. DeLucia, A.W. Schoettle and H. Smolander. 1995. Photosynthetic light capture and processing from cell to canopy. *In* Resource Physiology of Conifers. Eds. W.K. Smith and T.M. Hinckley. Academic Press, New York, pp 3–38.

Sullivan, J.H., B.D. Bovard and E.M. Middleton. 1997. Variability in leaf-level CO_2 and water fluxes in *Pinus banksiana* and *Picea mariana* in Saskatchewan. Tree Physiol. 17:8–9.

Williams, M., E.B. Rastetter, D.N. Fernandes, M.L. Goulden, S.C. Wofsy, G.R. Shaver, J.M. Melillo, J.W. Munger, S.-M. Fan and K.J. Nadelhoffer. 1996. Modelling the soil-plant-atmosphere continuum in a *Quercus–Acer* stand at Harvard Forest: the regulation of stomatal conductance by light, nitrogen and soil/plant hydraulic properties. Plant Cell Environ. 19:911–927